

See discussions, stats, and author profiles for this publication at: <https://www.researchgate.net/publication/269702121>

Surfactant Promoted Synthesis of CuCr₂O₄ Spinel Nanoparticles: A Recyclable Catalyst for One-Pot Synthesis of Acetophenone from Ethylbenzene

ARTICLE *in* INDUSTRIAL & ENGINEERING CHEMISTRY RESEARCH · DECEMBER 2014

Impact Factor: 2.59 · DOI: 10.1021/ie5026634

CITATIONS

2

READS

76

3 AUTHORS:



[Shankha Shubhra Acharya](#)

Indian Institute of Petroleum (IIP)

33 PUBLICATIONS 175 CITATIONS

[SEE PROFILE](#)



[Shilpi Ghosh](#)

29 PUBLICATIONS 151 CITATIONS

[SEE PROFILE](#)



[Rajaram Bal](#)

Indian Institute of Petroleum (IIP)

69 PUBLICATIONS 681 CITATIONS

[SEE PROFILE](#)

Surfactant Promoted Synthesis of CuCr₂O₄ Spinel Nanoparticles: A Recyclable Catalyst for One-Pot Synthesis of Acetophenone from Ethylbenzene

Shankha S. Acharyya,[†] Shilpi Ghosh,[†] and Rajaram Bal*

Catalytic Conversion & Processes Division, CSIR-Indian Institute of Petroleum, Dehradun-248005, India

 Supporting Information

ABSTRACT: We report a facile hydrothermal synthesis method to prepare CuCr₂O₄ spinel catalyst nanoparticles 20–60 nm in size, mediated by cationic surfactant cetyltrimethylammonium bromide. Detailed characterization of the material was carried out by X-ray diffraction (XRD), X-ray photoelectron spectroscopy (XPS), scanning electron microscopy (SEM), transmission electron microscopy (TEM), thermogravimetric analysis (TGA), Fourier transform infrared (FTIR) spectroscopy, and inductively coupled plasma–atomic emission spectroscopy (ICP-AES). XRD analysis revealed the formation of a CuCr₂O₄ spinel phase and TEM analysis showed that the particle size was 20–60 nm. The catalyst was highly active for selective oxidation of ethylbenzene to acetophenone with H₂O₂. The influence of reaction parameters such as temperature, substrate-to-oxidant molar ratio, reaction time, etc. were investigated in detail. The reusability of the catalyst was tested by conducting same experiments with the spent catalyst, and it was found that the catalyst did not show any significant activity loss, even after five cycles of reuse. An ethylbenzene conversion of 68.5% with 78% acetophenone selectivity was achieved over this catalyst at a temperature of 70 °C. However, significant H₂O₂ decomposition takes place on the catalyst, necessitating its usage in 5-fold excess.

1. INTRODUCTION

The selective oxidation of saturated hydrocarbons to the corresponding oxygenates is among the most important and challenging reactions in the chemical industry.^{1,2} Recently, the selective oxidation of ethylbenzene to acetophenone has drawn immense attention, because the acetophenone serves as a crucial platform as it is used as an intermediate for the manufacture of some perfumes, pharmaceuticals, resins, alcohols, esters, and aldehydes.^{3–5} Conventionally, acetophenone is synthesized by Friedel–Crafts acylation of arenes by acyl halides or acid anhydrides with Lewis acids or by oxidation of alkylarenes with stoichiometric inorganic oxidants such as permanganate or dichromate.^{6–8} However, these reagents are not only relatively expensive, but they also produce huge amounts of noxious and corrosive wastes. Moreover, it is difficult to separate the catalysts from the reaction mixture. Many researchers came forward to take war-footing steps against these problems and reported acetophenone production from ethylbenzene using several oxidants, such as TBHP,^{9,10} H₂O₂,¹¹ and molecular O₂.^{12,13} Recently, Chen et al. reported oxidation of ethylbenzene over Co-SiO₂-based nanocomposite catalyst¹⁴ and Luo et al. reported oxidation of ethylbenzene using carbon nanotubes with air as an oxidant.¹⁵ But, so far and so forth, none of the reported processes have been developed, largely because either high reaction temperatures have been employed or poor selectivity of acetophenone was observed, despite higher conversion, or severe leaching of the catalyst was observed. Therefore, there is substantial interest in the development of more efficient, readily separable, reusable catalysts for the catalytic oxidation of ethylbenzene. H₂O₂ is an economically and environmentally desirable oxidant in comparison to other oxidants.¹⁶ In addition, the activated C–H bonds (that is, adjacent to a heteroatom, a π-system and/or

an electron-rich tertiary C–H bond) are hydroxylated selectively by H₂O₂ in most metal-catalyzed oxidation systems.¹⁶

Copper chromite composite oxide is a versatile catalyst and has been employed as a catalyst for chemical reactions such as hydrogenation, dehydrogenation, oxidation, alkylation, etc. and thus find a wide range commercial applications.^{17–19} Moreover, copper chromite finds its major application as a burn rate modifier in solid propellant processing for space launch vehicles globally.^{20–22} Studies have shown that copper chromite has been considered the most effective catalyst, because of the tetragonally distorted normal spinel structure with $c/a < 1$ and the arrangement of copper in its structure.²³ In our previous report, we showed the preparation of CuCr₂O₄ spinel nanoparticles catalyst using nitrate²⁴ and chloride²⁵ precursors of copper and chromium for the selective oxidation of toluene²⁴ and oxidative coupling of aniline,²⁵ respectively. However, the catalyst has not been well explored for the selective catalytic oxidation of ethylbenzene by virtue of benzylic C^{sp₃}–H activation, which is considered as a challenging topic in contemporary chemical research.

Herein, we report the cationic surfactant CTAB-promoted, hydrothermal-based preparation of CuCr₂O₄ spinel nanoparticles catalyst, using the sulfate precursors of copper and chromium. We obtained thoroughly dispersed CuCr₂O₄ spinel nanoparticles, which were hardly obtained using nitrate and chloride precursors.^{24–26} We also report here the catalytic application of the CuCr₂O₄ spinel nanoparticles on the

Received: July 4, 2014

Revised: November 18, 2014

Accepted: December 9, 2014

oxidation of ethylbenzene at liquid phase with H_2O_2 as an oxidant. An ethylbenzene conversion of 68.5% with an acetophenone selectivity of 78% was achieved over this catalyst. To the best of our knowledge, there is no report on acetophenone production with high yield using H_2O_2 as an oxidant.

2. EXPERIMENTAL SECTION

The CuCr_2O_4 spinel nanoparticles catalyst was prepared hydrothermally, modifying our own preparation method.^{24–26}

2.1. Materials. Copper sulfate [$\text{CuSO}_4 \cdot 5\text{H}_2\text{O}$, Sigma-Aldrich] and chromium sulfate [$\text{Cr}_2(\text{SO}_4)_3 \cdot 12\text{H}_2\text{O}$, Sigma-Aldrich] were used as precursors for the preparation of CuCr_2O_4 nanoparticles. Other chemicals included anhydrous ethanol, cetyltrimethylammonium bromide, ammonium hydroxide, hydrazine hydrate (80% aqueous solution), ethylbenzene (purity >99.9%), acetonitrile (HPLC grade), and deionized water. All of these chemicals were bought from Sigma-Aldrich Co. Hydrogen peroxide was bought from (50 wt % in H_2O) Merck KGaA, Darmstadt, Germany. All chemicals were used as received without further purification.

2.2. Catalyst Preparation. In a typical synthesis, 1.0 g $\text{CuSO}_4 \cdot 5\text{H}_2\text{O}$ and 5.0 g of $\text{Cr}_2(\text{SO}_4)_3 \cdot 12\text{H}_2\text{O}$ at a desired molar ratio (Cu:Cr = 1:2) were dissolved in 118 g of water (mixed with 10 wt % ethanol) to give a clear dark blue solution. The pH of solutions was measured by pH Meter Eutech, which was standardized for pH measurement prior to use. The pH of the solution was adjusted to 8 by gradual addition of aqueous ammonia solution. After adding 0.75 g of cetyltrimethylammonium bromide to the solution, a dark green transparent gel formed within a few minutes. Next, 0.3 g of hydrazine hydrate solution was added dropwise to the resultant gel to produce a brown-colored coffee-like gel. The reagents were added maintaining the molar ratio of Cu:Cr:CTAB:H₂O:hydrazine = 1:2:0.5:200:1. The obtained wet gel was aged under air atmosphere for 1 h (40 °C) and subsequently sealed in a Teflon-lined stainless steel autoclave (treated hydrothermally under autogenous pressure) for 18 h at 180 °C. After that, the autoclave was allowed to cool until it reaches room temperature. The green fluffy solid products (precipitates) were collected by centrifugation at 5000 rpm and washed with water and ethanol several times prior to drying in air at 100 °C for 6 h. The resulting dry powder was transferred to a quartz reactor inside a tubular resistance furnace for calcination. The calcination was operated at 750 °C for 6 h under oxygen atmosphere at a ramp of 1 °C min. The obtained black powder was stored for further characterization.

2.3. Liquid-Phase Hydroxylation. Liquid-phase oxidation reaction was carried out in a two-neck round-bottom flask, equipped with refrigerant, containing 0.05 g of catalyst, 10 mL of solvent (acetonitrile), and 1 g of ethylbenzene to which H_2O_2 (50% aqueous solution) was added dropwise to prevent immediate H_2O_2 decomposition. The flask was then emerged in a preheated oil bath and vigorously stirred with a magnetic stirrer. The reaction temperature was ranged between room temperature (RT) and 90 °C. Small aliquots of the sample were withdrawn from the reaction mixture at regular intervals for analysis using a syringe. At the end of the reaction, the solid particles (catalyst) were separated by filtration and the products were analyzed by gas chromatography (GC) (Agilent, Model 7890) connected with a HP5 capillary column (30 m length, 0.28 mm id, 0.25 μm film thickness) and flame ionization detection (FID) device. Chem Station software was used to

collect and analyze the respective GC data. The relative error of product determination did not exceed ±5%. The benzene conversion and phenol formation were calculated using a calibration curve (obtained by manual injecting the authentic standard compounds). An anisole solution with a known amount was used as an external standard for analysis. The individual yields were calculated and normalized with respect to the GC response factors. The product identification was carried out by injecting the authentic standard samples in GC and GC-MS. For the reusability test, the catalyst was repeatedly washed with acetonitrile and acetone and dried overnight at 110 °C and used as such, without regeneration. In order to check the metal leaching, the mother liquor was then analyzed using ICP-AES.

2.4. Material Balance. We have performed the carbon balance for the most of the experiments and have also done the material balance for few experiments. The estimated error in analysis arising due to sampling and handling losses was ±5%.

3. RESULTS AND DISCUSSION

3.1. Characterization. The resulting X-ray diffraction (XRD) profiles were analyzed to identify the crystal phase of the catalyst using reference standards. The XRD patterns of the Cu-Cr catalysts are presented in Figure 1. XRD pattern

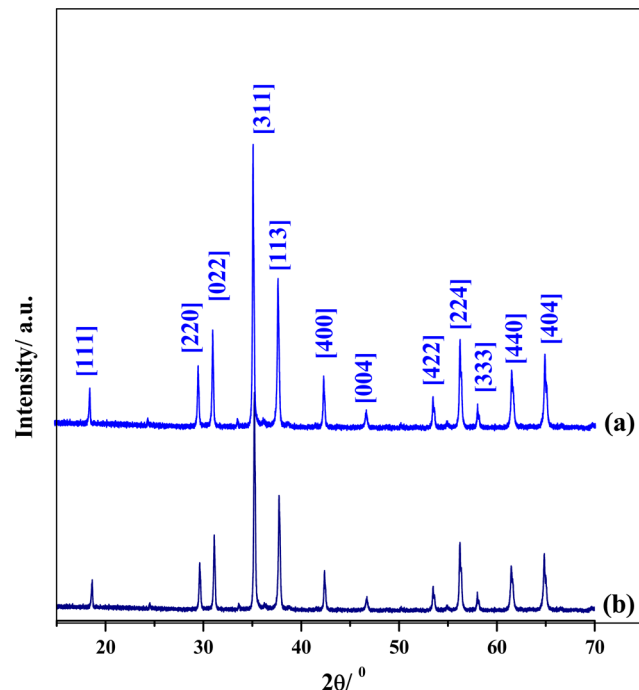


Figure 1. XRD diffractogram of (a) fresh and (b) spent CuCr_2O_4 spinel nanoparticle catalyst.

showed the typical diffraction lines of the bulk, single-phase CuCr_2O_4 spinel (Figure 1) (JCPDS File Card No. 05-0657) with maximum intensity peak at $2\theta = 35.16^\circ$. No impurity phase such as CuCrO_2 and not even cubic or monoclinic CuCr_2O_4 was found. The particle size was determined from the full width at half maxima (fwhm) of the line broadening corresponding to the diffraction angle of 35.16°, using the Debye-Scherrer equation, and a mean particle size (crystallite size) of 38 nm was observed. XRD diffractograms (Figure 1b) also predict that the catalyst retains its spinel phase, even after five recycles. The catalyst surface composition and oxidation state were investigated by XPS (Figure S1 in the Supporting

Information), which revealed that the surface of the catalyst is comprised of copper (valence of +2) and chromium (valence of +3). The CuCr_2O_4 spinel nanoparticles catalyst, prepared hydrothermally in the presence of cetyltrimethylammonium bromide (CTAB) surfactant, showed a single-phase morphology reflecting an assembly effect of the surfactant as imaged by SEM (Figure 2). SEM images of the catalyst (Figure 2) showed

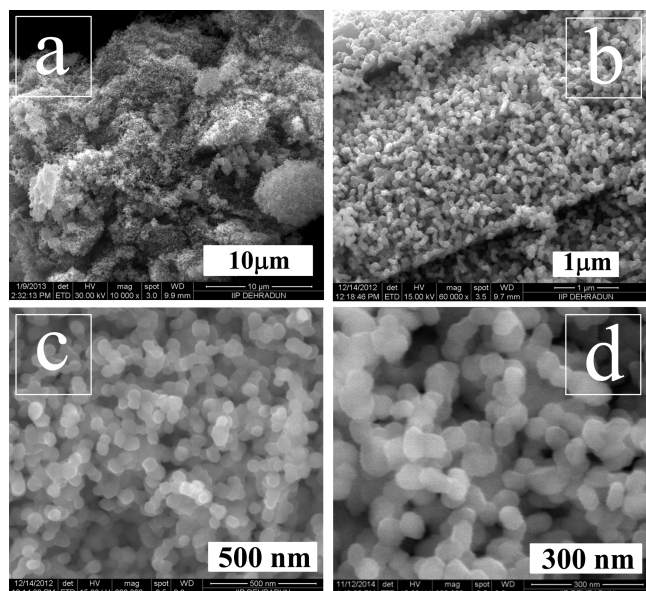


Figure 2. SEM images of CuCr_2O_4 spinel nanoparticle catalyst with successively higher magnifications.

the formation of almost homogeneously distributed uniform particles 20–60 nm in size, and was entirely different from that of the commercial catalyst, which is composed of larger and nonuniform particles (as evident from its SEM image, shown in Figure S2 in the Supporting Information). Thus, the structure-directing effect of CTAB is clearly evident from the SEM analysis. From the EDAX image, it can be seen that the sample contains only Cu, Cr, and O and the elemental mapping demonstrated the homogeneous distribution of Cu and Cr in the catalyst (Figure 3b). The embedding of CTAB molecules on the precalcined catalyst surface was further confirmed from TGA analysis (see Figure 4) and Fourier transform infrared

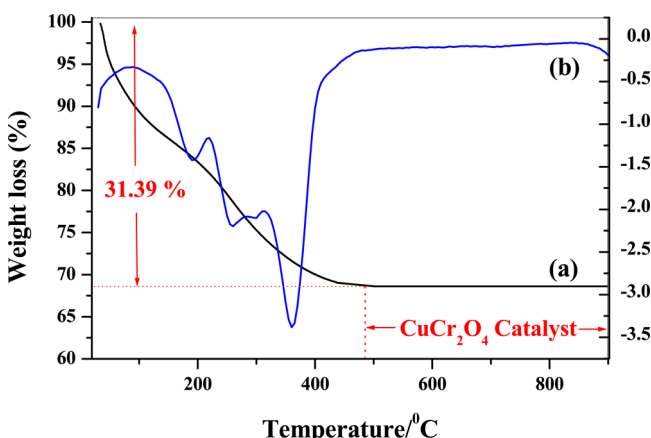


Figure 4. (a) TGA and (b) DTG analyses of the uncalcined CuCr_2O_4 spinel nanoparticle catalyst.

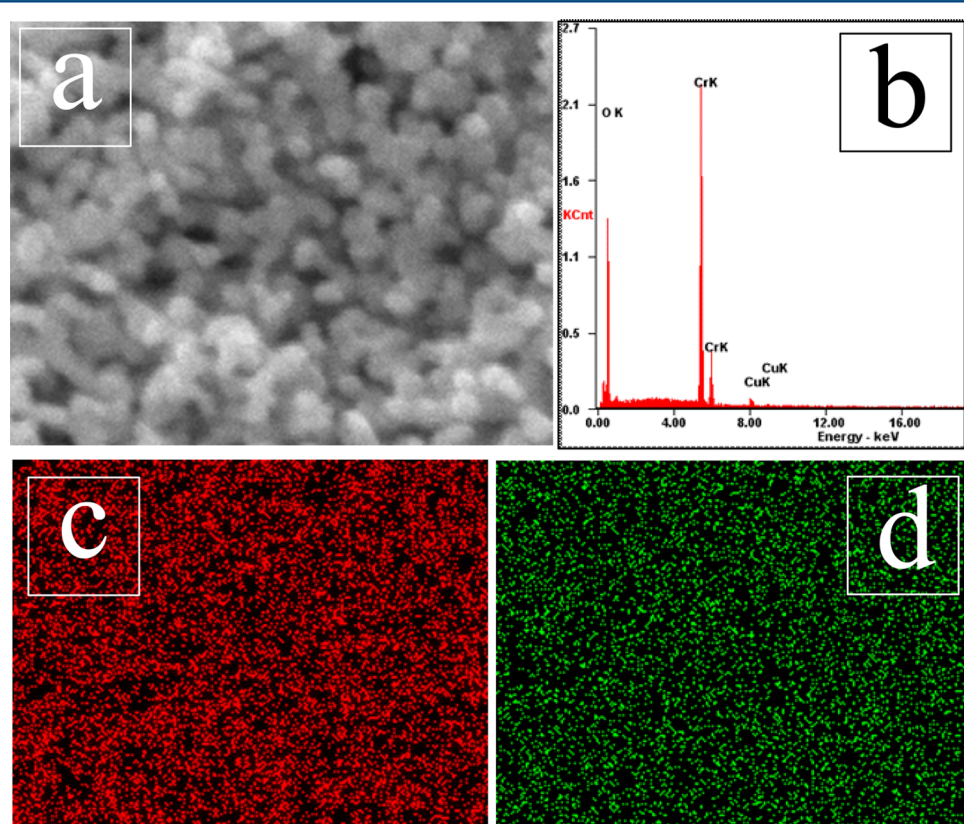


Figure 3. Elemental-mapping (based on Figure 2d) of (c) Cu and (d) Cr in a CuCr_2O_4 spinel nanoparticle catalyst.

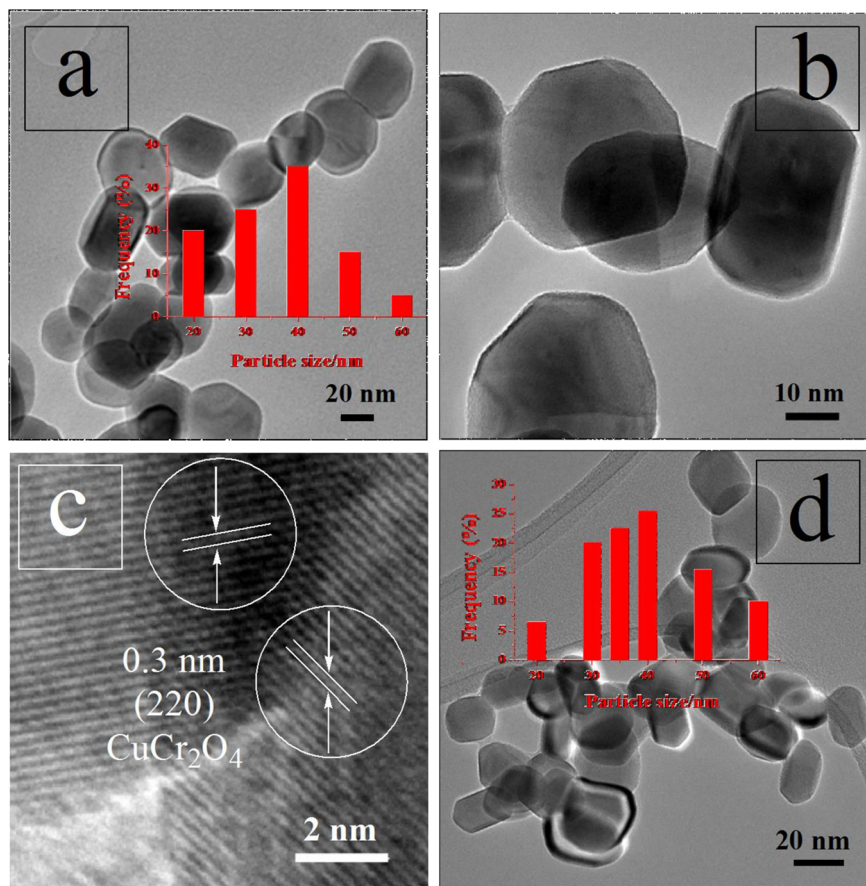


Figure 5. TEM images of the (a–c) fresh and (d) spent CuCr_2O_4 spinel nanoparticle catalyst.

Table 1. Activities of the Different Catalysts for Ethylbenzene Oxidation^a

entry	catalyst	$C_{\text{EB}} (\%)^b$	$S_p (\%)^c$					$Y_{\text{AP}} (\%)^d$	$E_0 (\%)^e$
			AP	${}^p\Phi_{\text{OH}}$	${}^o\Phi_{\text{OH}}$	PE	others		
1	CuO^{COM}	3.5	25.5	22	15	10	27.5	0.9	0.2
2	$\text{Cu}_2\text{O}^{\text{COM}}$	2.8	15	19	12.5	8	45.5	0.4	0.08
3	$\text{Cr}_2\text{O}_3^{\text{COM}}$	3.5	18	27	10	7.5	37.5	0.6	0.1
4	$\text{CuCr}_2\text{O}_4^{\text{COM}}$	6.5	48	18	12	7	15	3.1	0.6
5	$\text{CuO-Cr}_2\text{O}_3^{\text{IMP}}$	5.5	32	15	8	7	38	1.8	0.4
6 ^f	$\text{CuO-Cr}_2\text{O}_3$	35	55	18	8	4	15	19.25	3.9
7 ^g	$\text{CuCr}_2\text{O}_4^{\text{NP}}$	68.5	78	11.5	4.5	2.5	3.5	53.4	10.7
8 ^h	$\text{CuCr}_2\text{O}_4^{\text{NP}}$	66.8	75	13	4	3	5	50.1	10
9 ⁱ	$\text{CuCr}_2\text{O}_4^{\text{NP}}$								
10	no catalyst								

^aTypical reaction conditions: solvent (MeCN), 10 mL; substrate (ethylbenzene), 1 g; catalyst, 0.05 g; benzene:H₂O₂ molar ratio, 1:5; reaction temperature, 70 °C; and time, 6 h. ^b C_{B} represents the conversion of ethylbenzene, based on the FID-GC using methanol as the external standard ($C_{\text{B}} = [\text{moles of ethylbenzene reacted}/\text{initial moles of ethylbenzene used}] \times 100$). ^c S_p represents the selectivity to acetophenone ($S_p = [\text{moles of products produced}/\text{moles of ethylbenzene reacted}] \times 100$). ^d Y_{AP} represents the yield of acetophenone ($Y_{\text{AP}} = C_{\text{EB}} \times S_{\text{AP}}/100$). ^e E_0 represents the H₂O₂ efficiency ($E_0 = [\text{moles of phenol formed}/\text{total moles of H}_2\text{O}_2 \text{ added}] \times 100$). ^fCu-nanoclusters supported on Cr₂O₃. ^gPrepared CuCr₂O₄ spinel nanoparticles. ^hCatalyst after five cycles of reuse. ⁱUsing 2,6-di-*tert*-butyl-4-methyl phenol as radical scavenger. COM: commercial; IMP: impregnation method; CPM: coprecipitation method; NP: nanoparticles.

(FTIR) analysis (see Figure S3 in the Supporting Information). TGA-DTG analyses (Figure 4) were carried out to understand the various weight-loss regimes of the uncalcined catalyst. Three discrete regions of thermal decomposition can be observed in the DTG curve: the first weight loss corresponds to the elimination of water, followed by the decomposition of reactants to form NO_x and organic phases at 150–230 °C, and, finally, the combustion process, which occurs between 250 °C

and 330 °C. A further mass loss is noticed between 350 °C and 450 °C, because of the elimination of the remaining carbon and organic compounds. This region is likely due to the formation of a crystallized Cu–Cr–O inorganic phase and the release of lattice oxygen. Further weight loss was not observed when the temperature was further increased from 500 °C to 800 °C; no weight loss was expected, indicating the formation of stable CuCr₂O₄ spinel catalyst in that temperature zone.²⁷

The representative transmission electron microscopy (TEM) of the catalyst is shown in Figure 5. The TEM image showed that the catalyst was comprised of an almost uniform type of particles. The particle size distribution histogram (based in Figure 5a) demonstrates that major of the CuCr_2O_4 particles are in the size range of 20–60 nm (Figure 5a, inset). The lattice fringe with a d -spacing of 0.30 nm, corresponding to the [220] plane of CuCr_2O_4 spinel with a diffraction angle (2θ) of 29.6°, is also presented (Figure 5c).²⁰ From the TEM analysis, we can conclude that the [220] plane is the exposed plane, which may be active for the catalysis. The TEM image of the spent catalyst (after 5 recycles) has been shown in Figure 5d. The particle size distribution histogram (based in Figure 5d) also showed that major particles of the spent catalyst lie in the 20–60 nm size zone. The TEM images of the catalyst revealed that the particle size of the CuCr_2O_4 spinel was almost unchanged during the catalysis in terms of their morphology and particle sizes.

3.2. Catalytic Activities of the Catalyst. The activities of CuCr_2O_4 spinel nanoparticles ($\text{Cu}-\text{Cr}^{\text{NP}}$) catalyst in the direct oxidation of ethylbenzene to acetophenone in liquid phase by using H_2O_2 as an oxidant have been summarized in Table 1. Main product was detected to be acetophenone (AP). Main byproducts were detected to be *p*-hydroxy ethylbenzene (${}^p\Phi_{\text{OH}}$), *o*-hydroxy ethylbenzene (${}^o\Phi_{\text{OH}}$), and a very small amount of 1-phenylethanol (PE). Oxidation of ethylbenzene was speculated to occur in two different pathways: one is the aromatic ring hydroxylation and other is the side chain oxidation at primary and secondary carbon atoms. At room temperature (35 °C), the poor conversion of ethylbenzene conversion was noticed, although the selectivity to acetophenone was >80%. At higher temperatures (>50 °C), although the conversion of ethylbenzene increased, the selectivity to acetophenone was noticed to be sharply decreasing, because of the formation of *p*- and *o*-hydroxyl ethylbenzenes (Figure 6). Therefore, it can be assumed rationally that activation in the aromatic ring occurs at higher temperatures. To maintain the

higher selectivity of acetophenone, we tried to carry out the reactions at moderate temperature (at 70 °C), where we also expected the satisfied conversion of ethylbenzene. We then varied different reaction conditions to achieve a higher yield of acetophenone at 70 °C. When the ethylbenzene: H_2O_2 molar ratio was low (for example, 1:1 or 1:3), we observed a low conversion of ethylbenzene; moreover, the selectivity of acetophenone also was not up to the mark (Figure 7), probably

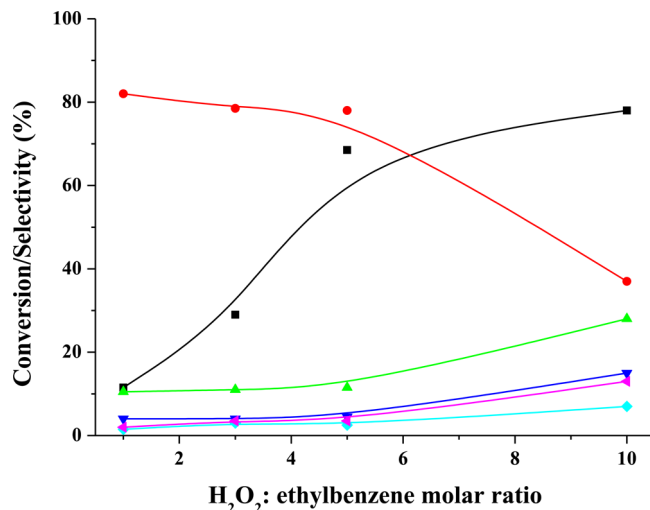


Figure 7. Effect of H_2O_2 :ethylbenzene molar ratio on ethylbenzene oxidation. Reaction conditions: ethylbenzene, 1 g; catalyst weight, 0.05 g; temperature, 70 °C; and time, 6 h. [Legend: (black square, ■) conversion of ethylbenzene; (red circle, ●) selectivity to acetophenone; (green triangle, ▲) selectivity to *p*-hydroxy ethylbenzene; (dark blue inverted triangle, ▼) selectivity to *o*-hydroxy ethylbenzene; (light blue diamond, ♦) selectivity to 1-phenyl ethanol; (purple left-facing triangle, ◀) selectivity to others.]

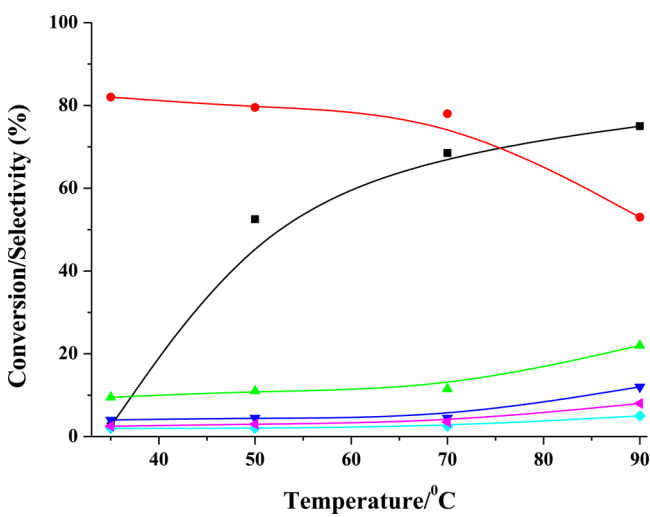


Figure 6. Effect of temperature on ethylbenzene oxidation. Reaction conditions: ethylbenzene, 1 g; catalyst, 0.05 g; ethylbenzene: H_2O_2 molar ratio, 1:5; and time, 6 h. [Legend: (black square, ■) conversion of ethylbenzene; (red circle, ●) selectivity to acetophenone; (green triangle, ▲) selectivity to *p*-hydroxy ethylbenzene; (dark blue inverted triangle, ▼) selectivity to *o*-hydroxy ethylbenzene; (light blue diamond, ♦) selectivity to 1-phenyl ethanol; and (purple left-facing triangle, ◀) selectivity to others.]

due to inevitable decomposition of H_2O_2 at that temperature over the catalyst. A blank reaction was performed (entry 10, Table 1) without any catalyst; the conversion of ethylbenzene was too poor to be detected, reflecting the necessity of the catalyst in this oxidation reaction. We also observed that an increment in catalyst weight decreased the selectivity of acetophenone (Figure 8), probably because the increase in more-active catalytic sites facilitated the attacking positions of ethylbenzene in all of its possible sites. Maintaining all the optimum conditions, when the reaction was allowed to run for hours (Figure 9), we noticed that, although the conversion of ethylbenzene increased with time, the acetophenone selectivity gradually decreased, because of the formation of *p*- and *o*-hydroxyacetophenones, phenylacetaldehyde, and benzaldehyde (included in “others”).

Notably, commercial Cr_2O_3 , CuO , Cu_2O , and CuCr_2O_4 catalyst did not show any activity (see entries 1–4, Table 1). Conventional catalyst prepared via the impregnation method also showed negligible activity (entry 5, Table 1). The reason can be attributed to the small size as well as extreme stable spinel phase, containing nonleachable species. The comparatively smaller size of CuCr_2O_4 spinel nanoparticles catalyst possess comparatively high specific surface area, which corresponds to higher dispersion of the catalyst, which leads to the availability of more exposed surface-active sites, where the catalytic reaction takes place. Inevitably, a higher reaction rate was observed in the case of the CuCr_2O_4 spinel

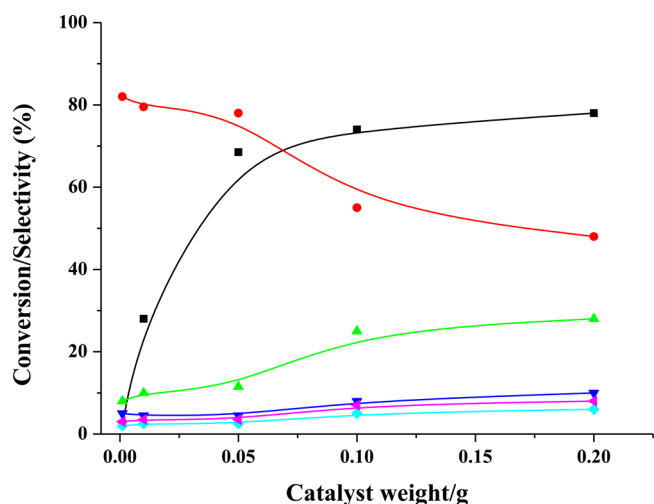


Figure 8. Effect of catalyst weight on ethylbenzene oxidation. Reaction conditions: ethylbenzene, 1 g; ethylbenzene:H₂O₂ molar ratio, 1:5; temperature, 70 °C; and time, 6 h. [Legend: (black square, ■) conversion of ethylbenzene; (red circle, ●) selectivity to acetophenone; (green triangle, ▲) selectivity to *p*-hydroxy ethylbenzene; (dark blue inverted triangle, ▽) selectivity to *o*-hydroxy ethylbenzene; (light blue diamond, ♦) selectivity to 1-phenyl ethanol; (purple left-facing triangle, ◁) selectivity to others.]

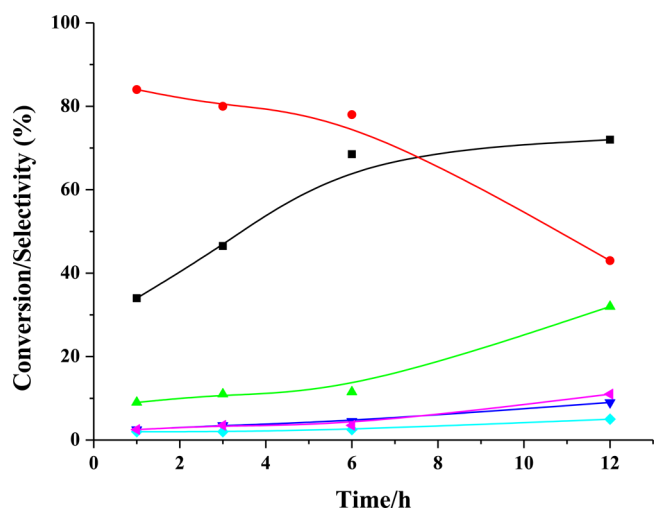


Figure 9. Effect of time-on-stream on ethylbenzene oxidation. Reaction conditions: ethylbenzene, 1 g; catalyst weight, 0.05 g; ethylbenzene:H₂O₂ molar ratio, 1:5; and temperature, 70 °C. [Legend: (black square, ■) conversion of ethylbenzene; (red circle, ●) selectivity to acetophenone; (green triangle, ▲) selectivity to *p*-hydroxy ethylbenzene; (dark blue inverted triangle, ▽) selectivity to *o*-hydroxy ethylbenzene; (light blue diamond, ♦) selectivity to 1-phenyl ethanol; (purple left-facing triangle, ◁) selectivity to others.]

nano-particles catalyst. The poor catalytic activity of the impregnated catalyst may be attributed to their irregular shape and larger particle size, which limits the accessibility of the catalyst toward the reacting substrates. Although nano-clusters of Cu(II) supported on nanocrystalline Cr₂O₃ meet this criteria, the catalyst suffers severe leaching and, thus, its use is limited in ethylbenzene oxidation reaction.

We have plotted H₂O₂ consumption, in terms of its efficiency (E_0) in Table 1. The E_0 values also depict that only the CuCr₂O₄ spinel nanoparticles catalyst effectively utilized H₂O₂ and compelled it to react selectively. This also reflects,

indirectly, the fact that the CuCr₂O₄ spinel nanoparticle catalyst has superior catalytic activity, compared to the conventional and commercial catalysts.

The oxidation of ethylbenzene over CuCr₂O₄ spinel nanoparticle catalyst by H₂O₂ probably proceeds via the involvement of a peroxyradical intermediate.¹¹ The peroxyradical intermediate generated over CuCr₂O₄ surface is stabilized to a great extent by acetonitrile solvent²⁸ and is able to oxyfunctionalize the side chain (ethyl group) at the primary and secondary C atoms, leading to the formation of the corresponding carbinols. These carbinols undergo further oxidation to the respective aldehyde (phenyl acetaldehyde) and ketone (acetophenone). Moreover, dissociation of H₂O₂ generates hydroxy radicals²⁹ that act as electrophiles and approach the benzene nucleus and produces *o*- and *p*-hydroxy ethylbenzenes.³⁰ This explains the decreased selectivity of acetophenone with increasing amounts of H₂O₂. Furthermore, aromatic ring hydroxylation at the *p*-position is preferred, to some extent, compared to the *o*-position and thus detected to be present in greater amount than its *o*-analogue. We also noticed that 1-phenylethanol was produced in much smaller amounts, comparatively, in all experiments (i.e., the side chain oxidation at the secondary carbon dominates over the primary C atom). This phenomenon can be explained on the basis of the existence of a barrier to rotation about the C_{sp₂}–C_{sp₃} bond present in ethylbenzene.³¹ The methyl groups (terminal) in ethylbenzene rotate more rapidly than the methylene group; hence, it is very much resistant to attack by active species generated by H₂O₂.

The efficiency of a heterogeneous catalyst is evaluated in terms of its recyclability and stability. The reusability of the catalyst CuCr₂O₄ was studied without any regeneration. After each run, the catalyst was filtered during hot conditions, repeatedly washed with acetonitrile and acetone, and dried overnight at 100 °C, and then was used as such. We observed that the CuCr₂O₄ catalyst showed negligible change in its activity (see entry 8, Table 1 and Figure 10). The amount of Cu and Cr present in CuCr₂O₄ catalyst after five cycles of reuse was almost same as the fresh catalyst (estimated by ICP-AES), confirming the true heterogeneity of the catalyst. After five

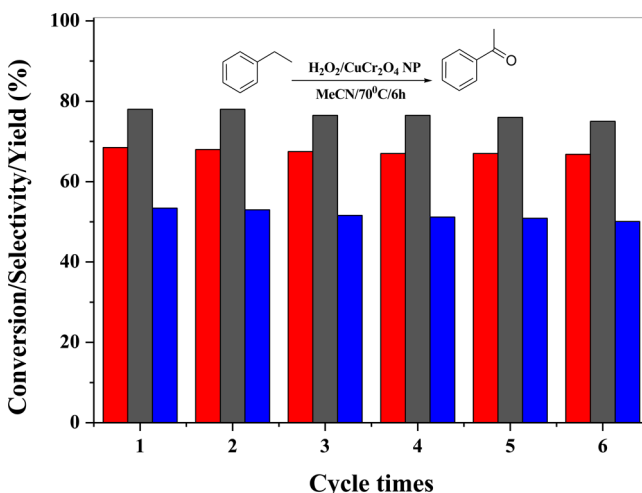


Figure 10. Recyclability tests of CuCr₂O₄ spinel nanoparticles catalyst for the oxidation reaction of ethylbenzene to acetophenone. [Legend: (red) conversion of ethylbenzene, (black) selectivity to acetophenone, and (blue) yield of acetophenone.]

recycles, a negligible amount of leaching of Cu and Cr was detected by ICP-AES (the concentrations of both metals were <2 ppb).

4. CONCLUSIONS

In summary, we have developed a surfactant-promoted simple preparation method to prepare 25–50 nm CuCr₂O₄ spinel nanoparticles having high thermal stability and good catalytic activity for the single-step conversion of ethylbenzene to acetophenone using H₂O₂, exhibiting 68.5% ethylbenzene conversion and 78% selectivity toward acetophenone at 70 °C. The catalyst can be reused several times without any activity loss. The proposed method is also advantageous from the standpoint of low cost, environmental benignity, and operational simplicity; furthermore, it can be applicable to large-scale reactions. This environmentally benign, “green” route to acetophenone production may be a potential alternative to the existing process.

■ ASSOCIATED CONTENT

Supporting Information

Detailed experimental procedure, catalyst-characterization techniques, SEM-EDAX, elemental mapping, XPS, TGA diagram, graphical presentation of effects of different reaction parameters on ethylbenzene oxidation etc. This material is available free of charge via the Internet at <http://pubs.acs.org>.

■ AUTHOR INFORMATION

Corresponding Author

*Tel.: +91 135 2525 917. Fax: +91 1352660202. E-mail: raja@iip.res.in.

Author Contributions

[†]These authors contributed equally.

Notes

The authors declare no competing financial interest.

■ ACKNOWLEDGMENTS

S.S.A. thanks CSIR and S.G. thanks UGC, New Delhi, India, for their respective fellowships. R.B. thanks CSIR, New Delhi, for financial support in the form of the 12 FYP Project (CSC-0125, CSC-0117). The Director, CSIR-IIP is acknowledged for his help and encouragement. The authors thank Analytical Section Division, IIP, for the analytical services.

■ ABBREVIATIONS

- CTAB = cetyltrimethylammonium bromide
- XPS = X-ray photoelectron spectroscopy
- XRD = X-ray diffraction
- SEM = scanning electron microscopy
- TEM = transmission electron microscopy
- TGA = thermogravimetric analysis
- DTG = differential thermogravimetry

■ REFERENCES

- (1) Gómez-Hortigüela, L.; Corà, F.; Catlow, C. R. A. Aerobic oxidation of hydrocarbons catalyzed by Mn-doped nanoporous aluminophosphates (IV): Regeneration mechanism. *ACS Catal.* **2011**, *1*, 1475–1486.
- (2) Li, X. H.; Chen, J. S.; Wang, X. C.; Sun, J. H.; Antonietti, M. Metal-free activation of dioxygen by graphene/g-C₃N₄ nanocomposites: Functional dyads for selective oxidation of saturated hydrocarbons. *J. Am. Chem. Soc.* **2011**, *133*, 8074–8074.
- (3) Qi, J. Y.; Ma, H. X.; Li, X. J.; Zhou, Z. Y.; Choi, M. C. K.; Chan, A. S. C.; Yang, Q. Y. Synthesis and characterization of cobalt(III) complexes containing 2-pyridinecarboxamide ligands and their application in catalytic oxidation of ethylbenzene with dioxygen. *Chem. Commun.* **2003**, 1294–1295.
- (4) Yang, G. Y.; Ma, Y. F.; Xu, J. Biomimetic catalytic system driven by electron transfer for selective oxygenation of hydrocarbon. *J. Am. Chem. Soc.* **2004**, *126*, 10542–10543.
- (5) Devika, S.; Palanichamy, M.; Murugesan, V. Selective oxidation of ethylbenzene over CeAlPO-5. *Appl. Catal., A* **2011**, *407*, 76–84.
- (6) Olah, G. A. *Friedel–Crafts and Related Reactions*, Vol. 2; Interscience Publishers: New York, 1963.
- (7) Clark, J. H.; Kybett, A. P.; Landon, P.; Macquarrie, D. J.; Martin, K. Catalytic oxidation of organic substrates using alumina supported chromium and manganese. *J. Chem. Soc. Chem. Commun.* **1989**, 1355–1356.
- (8) Lee, D. G.; Udo, A. Spitzer. Oxidation of ethylbenzene with aqueous sodium dichromate. *J. Org. Chem.* **1969**, *34*, 1493–1495.
- (9) Bennur, T. H.; Srinivas, D.; Sivasanker, S. Oxidation of ethylbenzene over “neat” and zeolite-Y-encapsulated copper tri- and tetraaza macrocyclic complexes. *J. Mol. Catal. A: Chem.* **2004**, *207*, 163–171.
- (10) Raji, V.; Chakraborty, M.; Parikh, P. A. Catalytic performance of silica-supported silver nanoparticles for liquid-phase oxidation of ethylbenzene. *Ind. Eng. Chem. Res.* **2012**, *51*, 5691–5698.
- (11) Mal, N. K.; Ramaswamy, A. V. Oxidation of ethylbenzene over Ti-, V- and Sn-containing silicates with MFI structure. *Appl. Catal., A* **1996**, *143*, 75–85.
- (12) Jana, S. K.; Wu, P.; Tatsumi, T. NiAl hydrotalcite as an efficient and environmentally friendly solid catalyst for solvent-free liquid-phase selective oxidation of ethylbenzene to acetophenone with 1 atm of molecular oxygen. *J. Catal.* **2006**, *240*, 268–274.
- (13) Devika, S.; Palanichamy, M.; Murugesan, V. Selective oxidation of ethylbenzene over CeAlPO-5. *Appl. Catal., A* **2011**, *407*, 76–84.
- (14) Chen, C.; Shi, S.; Wang, M.; Ma, H.; Zhou, L.; Xu, J. Superhydrophobic SiO₂-based nanocomposite modified with organic groups as catalyst for selective oxidation of ethylbenzene. *J. Mater. Chem. A* **2014**, DOI: 10.1039/c4ta00943f.
- (15) Luo, J.; Peng, F.; Yu, H.; Wang, H.; Zheng, W. Aerobic liquid-phase oxidation of ethylbenzene to acetophenone catalyzed by carbon nanotubes. *ChemCatChem.* **2013**, DOI: 10.1002/cctc.201200603.
- (16) Kamata, K.; Yonehara, K.; Nakagawa, Y.; Uehara, K.; Mizuno, N. Efficient stereo- and regioselective hydroxylation of alkanes catalysed by a bulky polyoxometalate. *Nat. Chem.* **2010**, *2*, 478–483.
- (17) Adkins, H.; Connor, R. The catalytic hydrogenation of organic compounds over copper chromite. *J. Am. Chem. Soc.* **1931**, *53*, 1091–1095.
- (18) Connor, R.; Folkers, K.; Adkins, H. The preparation of copper chromium oxide catalysts for hydrogenation. *J. Am. Chem. Soc.* **1932**, *54*, 1138–1145.
- (19) Roy, S.; Ghose, J. Synthesis and studies on some copper chromite spinel oxide composites. *Mater. Res. Bull.* **1999**, *34*, 1179–1186.
- (20) Kawamoto, A. M.; Pardini, L. C.; Rezende, L. C. Synthesis of copper chromite catalyst. *Aerosp. Sci. Technol.* **2004**, *8*, 591–598.
- (21) Jacobs, P. W. M.; Whitehead, H. M. Decomposition and combustion of ammonium perchlorate. *Chem. Rev.* **1969**, *69*, 551–590.
- (22) Armstrong, R. W.; Baschung, B.; Booth, D. W. Enhanced propellant combustion with nanoparticles. *Nano Lett.* **2003**, *3*, 253–255.
- (23) Sathiskumar, P. S.; Thomas, C. R.; Madras, G. Solution Combustion of nanosized copper chromite and its use as a burn rate modifier in solid propellants. *Ind. Eng. Chem. Res.* **2012**, *51*, 10108–10116.
- (24) Acharyya, S. S.; Ghosh, S.; Tiwari, R.; Sarkar, B.; Singha, R. K.; Pendem, C.; Sasaki, T.; Bal, R. Preparation of CuCr₂O₄ spinel nanoparticles catalyst for selective oxidation of toluene to benzaldehyde. *Green Chem.* **2014**, *16*, 2826–2834.

- (25) Acharyya, S. S.; Ghosh, S.; Bal, R. Catalytic oxidation of aniline to azoxybenzene over CuCr_2O_4 spinel nanoparticles catalyst. *ACS Sustainable Chem. Eng.* **2014**, *2*, 584–589.
- (26) Acharyya, S. S.; Ghosh, S.; Adak, S.; Sasaki, T.; Bal, R. Facile synthesis of CuCr_2O_4 spinel nanoparticles: A recyclable heterogeneous catalyst for one pot hydroxylation of benzene. *Catal. Sci. Technol.* **2014**, *4*, 4232–4241.
- (27) Li, W.; Cheng, H. Cu-Cr-O Nanocomposites: Synthesis and characterization as catalysts for solid state propellants. *Solid State Sci.* **2007**, *9*, 750–755.
- (28) Acharyya S. S.; Ghosh, S.; Bal, R. Direct oxyamination of benzene to aniline over Cu(II) nanoclusters supported on CuCr_2O_4 spinel nanoparticles catalyst via simultaneous activation of C–H and N–H bonds. *Chem. Commun.* **2014**, DOI: 10.1039/C4CC02937B.
- (29) Nagiev, T. M. *Coherent Synchronized Oxidation Reactions by Hydrogen Peroxide*; Elsevier: Amsterdam, 2006; ISBN: 978-0-444-52851-3.
- (30) Dubey, A.; Rives, V.; Kannan, S. *J. Mol. Catal. A: Chem.* **2002**, *181*, 151–160.
- (31) Schaefer, T.; Schurko, R. W.; Bernard, G. M. Does the C sp^2 —C sp^3 barrier in ethylbenzene have a hyperconjugative component? An indirect experimental and theoretical approach. *Can. J. Chem.* **1994**, *72*, 1780–1784.